IEEE Access
Multidisciplinary | Rapid Review | Open Access Journal

Received September 29, 2019, accepted October 23, 2019, date of publication October 28, 2019, date of current version November 7, 2019.

Digital Object Identifier 10.1109/ACCESS.2019.2949813

D2D Communication Underlaying UAV on Multiple Bands in Disaster Area: Stochastic Geometry Analysis

MOHAMED RIHAN[1,3], (Member, IEEE), MAHMOUD M. SELIM[2,4], (Member, IEEE), CHEN XU[1], AND LEI HUANG[2], (Senior Member, IEEE)

[1]School of Mathematics and Statistics, Shenzhen University, Shenzhen 518060, China
[2]School of Information Engineering, Shenzhen University, Shenzhen 518060, China
[3]Department of Electronics and Communication Engineering, Faculty of Electronic Engineering, Menoufia University, Menoufia 21974, Egypt
[4]Department of Electronics and Electrical Communications Engineering, Faculty of Engineering, Tanta University, Tanta 31511, Egypt

Corresponding author: Lei Huang (lhuang@szu.edu.cn)

This work was supported in part by the National Natural Science Foundation of China under Grant 61872429, Grant U1713217, and Grant U1501253, and in part by the Science and Technology Program of Shenzhen, China, under Grant JCYJ20170818091621856.

ABSTRACT When communication infrastructure is damaged due to natural disasters, employing unmanned aerial vehicle (UAV) as a flying base station (BS) and device-to-device (D2D) communication paradigms are among the essential strategies for seamless and reliable services. However, the communication reliability of the flying BS and the energy efficiency (EE) of the D2D communications may be degraded due to the shared spectrum coexistence of the UAV and D2D pairs. In this paper, we consider the uplink transmission to an UAV which is underlaid with D2D communication pairs randomly distributed on multiple frequency bands. For such a scenario, we derive tractable expressions for the successful transmission probability, the average sum-rate, and the EE of the network based on stochastic geometry principles, that perfectly match the simulation results. We also address the effects of D2D and UAV-connected users' densities on the EE and sum-rate as performance metrics in the uplink scenario. Finally, some critical insights are provided based on the trade-off between different network parameters, and accordingly recommendations are given for maximizing the EE of such networks in post-disaster situations.

INDEX TERMS Device-to-device (D2D), energy efficiency (EE), unmanned aerial vehicle (UAV), stochastic geometry, post-disaster.

I. INTRODUCTION

Unmanned aerial vehicles (UAVs) have gained considerable attention in the last few years due to its widely use in military, pubic and civil applications [1]. However, an exceptional importance is given to the applications of UAVs in the telecommunication sector. According to recent studies [2]–[9], UAVs are able to improve the quality-of-service (QoS), coverage, connectivity, reliability, and capacity of wireless communication networks [10]–[17]. Thanks to unique features of UAVs, i.e., ease of deployment, reprogramability during run-time, ability to hover and provide line-of-sight (LoS) connectivity, mobility, and flexibility [1]. One of the most important applications for UAVs is the support of communication networks during natural disasters [18]–[22]. Specifically, service providers can use UAVs as flying base stations (BSs) to provide temporary wireless connectivity to areas affected by the disaster.

Undoubtedly, UAVs can play a vital role in different communication scenarios, such as internet-of-things (IoT) [23], [24], device-to-device (D2D) communications [10], [18], [25], [26], emergency communications during disasters [18], and in fog or muli-access edge computing (MEC) networks [6], [27]. Zeng *et al.* [2] provide a taxonomy for the UAV-aided communication services into three categories, namely, UAV-aided relaying, UAV-aided ubiquitous coverage, and UAV aided information dissemination. A study on the optimum number of UAVs that can cover a specific service area has been accomplished through the spiral algorithm proposed by Lyu *et al.* [8]. Additionally, Mozaffari *et al.* [9], [10] proposed an algorithm based on the disc covering approach, through which they evaluate the optimum

The associate editor coordinating the review of this manuscript and approving it for publication was Wenchi Cheng.

number of stop points for a moving UAV to provide coverage for the whole service area. Khawaja *et al.* [28] present a comprehensive survey about the measurement methods and channel characterization efforts for low-altitude UAV channel modeling approaches. The adoption of millimeter-wave (mmWave) and beamforming techniques in UAV-assisted networks is studied in [30]. Furthermore, trajectory and hovering altitude optimization, also called as path-planning, as well as optimum deployment strategy were the core of many research works [6]–[11], [13], [16], [17].

Due to their unique features, UAVs have also been employed in emergency wireless networks for disaster relief operations [19]–[22]. In [19], a distributed and scalable architecture for UAV-assisted emergency wireless network has been proposed to convey messages to and from nodes in a wide disaster-affected regions. Erdelj and Natalizio [20] have proposed some services for disaster management that are mainly based on UAV-assisted communications. Moreover, Reina *et al.* [21] proposed a deployment strategy for UAVs in disasters, that is based on optimizing the positioning of UAVs upon a combination of global and local search algorithms. Furthermore, a path planning strategy of a flying UAV in post-disaster has been proposed by Christy *et al.* [22], where it takes into account the disaster conditions as well as some energy constraints.

With the growing deployments of UAVs due to their unique features and advantages, some technical challenges also arise. One of the most important challenges with the dense deployment of UAVs as flying BSs, is the harmful interference arising due to the use of the same spectrum bands by the flying UAV BSs as well as other wireless technologies. Additionally, two important challenges that might be very critical during disasters, are the energy constraint as well as coverage limitation. Specifically, the area affected by the disaster may be very large, but due to the limitation of battery energy, the UAV BS may not be able to provide wireless coverage for the whole area affected by the disaster. A key solution to deal with these critical challenges is the adoption of multi-hope D2D communications to effectively extend the wireless coverage of the UAV BS [6], [18], [23]–[26]. Generally, D2D communication paradigm allows the users to communicate directly with one another without any intervention from the BS or any system infrastructure [10]. Typically, the D2D communications operate in underlay fashion, where they share the same spectrum owned by a licensed user/system. However, this will give rise to many interference mitigation challenges [23]–[26]. In [31], the disaster affected areas which can not be covered directly by the UAV, may be covered by using multi-hop D2D links to relay the signals between mobile users and accordingly extend the coverage area and serve more users [32]. The resource allocation problem for D2D communication underlaying cellular network has been addressed by Feng *et al.* [33] through maximizing the overall network throughput under quality-of-service (QoS) constraints for the D2D users. Moreover, Lin *et al.* [34] optimized the D2D spectrum sharing of a tractable hybrid network model through optimizing a weighted proportional of traffic-type-based utility function. Furthermore, Zhang *et al.* [35] optimized the energy efficiency (EE) of the D2D communication underlaying cellular networks on multiple bands. Specifically, they maximize the EE of D2D underlaying cellular network on multiple bands under different coverage and QoS constraints. Nevertheless, this work lacks the use of UAV.

This article concentrates on studying the performance of uplink transmissions for users who are forced to temporarily communicate with UAV BS due to malfunctioning of their original terrestrial BSs. Moreover, the uplink cellular users are assumed to share multiple bands with other users who are involved in D2D communications. The main contributions in this article can be summarized as:

- Presenting a network planning solution for fast and reliable service recovery after severe disasters which can bring some neighboring BSs in the malfunction state. This planning solution depends on geometrically arranging each three neighboring cells in what is called *Johnson circles*. When severe disaster occurs, we propose implementing a single UAV flying BS that hovers at the central point of intersection of the cells to serve users who are involved in either cellular uplink or D2D communications. Fast service recovery can be managed through sending a single UAV BS to hover at a specific altitude determined on the lights of our results, which in turn send service recovery broadcast messages to users who are seeking for communication services. The reliability of the proposed planning strategy can be measured through the successful transmission probability of both uplink and D2D communications.
- For the proposed scenario above, exact expressions are derived for successful transmission probability, average sum-rate, and EE. In particular, we used the principles of stochastic geometry to analyze the performance of network assuming spectrum sharing over multi-bands between the UAV-connected uplink users and D2D users.
- Studying the interaction between different parameters, i.e, D2D user density, uplink user density, UAV altitude, and outage SINR thresholds for different kinds of users, and the impact of such parameters on different performance metrics, i.e. sum-rate and EE.

The rest of this article is organized as follows. In **Section** II, the system model of the UAV-assisted cellular network underlaid with D2D pairs is described. In **Section** III, the EE for both the D2D communications and UAV-assisted uplink transmissions are derived for the case where a single static UAV covers three neighboring service areas whose BSs are all malfunctioned. **Section** IV provides the detailed discussion of the simulation and numerical results. Finally, the paper is concluded in **Section** V.

II. SYSTEM MODEL

Consider a cellular network with three adjacent BSs and, due to a severe disaster that affects the whole area, a single

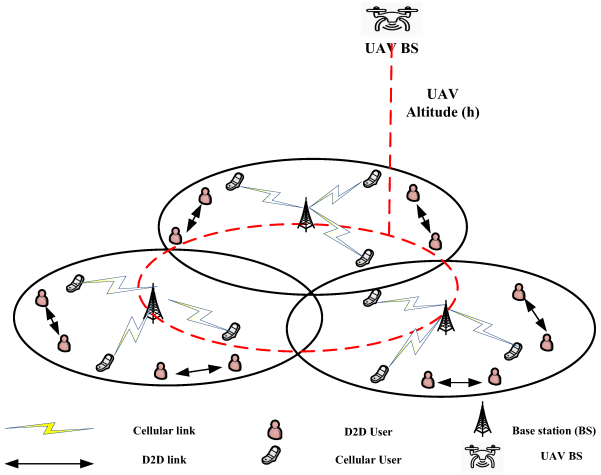

FIGURE 1. D2D communication underlaying UAV on multiple bands.

low-altitude[1] UAV will jointly serve the ground users as their flying BS. We assume that the three cells are circularly-shaped with the same radius R_c and the cells are managed so that there is no dead zone[2] between the cells, as shown in Fig. 1. Consider also that the whole cellular network is underlaid with D2D communication links, where the D2D communications share the uplink spectrum resources with the UAV that serves the whole three cells. The UAV is responsible for the resource allocation between the cellular and D2D users. Consider that the spectrum of the whole network is divided into K bands, and the bandwidth of the i^{th} band is W_i. From now on, the subscript i will be used to denote the i^{th} spectrum band and so that the subscript i can take the integer values from 1 to K. The users in this cellular system are either cellular users or D2D users. The cellular users are distributed within the cells according to a homogeneous Poisson point process (PPP) $\Phi_{c,i}$ with density[3] $\lambda_{c,i}$ (users $/m^2$) and the D2D users are distributed according to a homogeneous PPP $\Phi_{d,i}$, with density $\lambda_{d,i}$ (D2D pairs $/m^2$) [36], [37]. Note that, on each of the spectrum bands we could have both uplink users and D2D users sharing this band.

The arrangement of the three cells in the way mentioned above represents what is called *Johnson circles*. The three cells are three circles that are of the same radius R_c and share one common point of intersection. Note that the circles have a total of four intersections,[4] one of them is the common point that they all share, and for each of the three pairs of circles one more intersection point, namely 2-wise intersection. Here are some facts about the geometry of the proposed scenario:

- The centers of the circular cells lie on a circle with the same radius as the cells, R_c, such that its center is at the common point of intersection of the three cells.
- The 2-wise intersection points of the cells lie on a circle with also the same radius R_c.
- There is a circle of radius $2R_c$ centered at the common intersection point that covers the whole three cells and tangent each cell at only one point.

In the proposed scenario, the wireless channels are of two types, namely, the ground-to-ground(G2G) channel and the air-to-ground(A2G) channel. The term G2G channel refers to the channel between the D2D transmitter-receiver pairs. On the other hand, the uplink channel between any cellular user and the flying UAV BS, is an A2G channel. For the D2D communication links, we assume a Rayleigh fading channel model taking into account both the large-scale path-loss and the small-scale fading. Accordingly, the expression of the D2D received power P_r at the receiver due to the transmission of power P_t through the G2G channel can be expressed as $P_r = P_t R^{-\alpha} h$, where R stands for the distance between the transmitter and receiver of D2D pair, α is the path-loss exponent, and h refers to the Rayleigh fading coefficient that follows an independent exponential distribution with unit mean [29]. The received signal at any D2D receiver includes the desired signal from its transmitting pair, interference due to other D2D transmissions, and interference due to transmissions from the cellular users to the UAV BS. The UAV BS also receives the useful signal for each of the uplink cellular users and interference from all the D2D pairs. For easily following the mathematics in this paper, all symbols used throughout the paper are listed in **Table** 1.

The signal-to-interference-plus-noise ratio (SINR) for the l^{th} D2D receiver pair on the i^{th} band is expressed as:

$$\gamma_{d,l,i} = \frac{P^r_{d,l,i}}{I^c_{d,l,i} + I_{u,i} + N_0} \tag{1}$$

where $P^r_{d,l,i}$ is the power of the desired signal received from the l^{th} D2D pair transmitter, $I^c_{d,l,i}$ denotes the power of the interference signal due to the transmissions from other D2D pairs received at the l^{th} D2D pair receiver on the i^{th} band, $I_{u,i}$ corresponds to the interference due to the transmissions from users served directly by the UAV on the i^{th} band, and N_0 is the noise power. After normalizing the received signal powers as well as the noise power by the path-loss coefficient, we also have:

$$P^r_{d,l,i} = P^t_{d,i} R^{-\alpha_d}_{d,l,l} h_{l,l}, \tag{2}$$

$$I^c_{d,l,i} = \sum_{\substack{j \in \Phi_{d,i}, \\ j \neq l}} P^t_{d,i} R^{-\alpha_d}_{d,j,l} h_{j,l}, \tag{3}$$

where $h_{l,l}$ and $h_{j,l}$ refer to the channel gains between the transmitter and receiver of the l^{th} D2D pair, and the receiver of l^{th} D2D pair and the transmitter of the j^{th} D2D pair, respectively. $P^t_{d,i}$ is the D2D transmission power in the i^{th} band, which is assumed to be fixed for all D2D users,

[1]Low-alitiude UAV are platforms whose altitude lies between 300m - 1400m according to the application of interest.

[2]Dead-zone is the area that is not covered by any of the neighboring BSs.

[3]The user density can be defined as the average number of users within the region divided by the square area of that region in m^2, and accordingly, the average number of users in a region is equal to the density of users multiplied by the square area of that region.

[4]Intersections are points where at least two of the three circles meet.

TABLE 1. Key notations used in this paper.

Notation	Explanation
i	Index for the spectrum band of interest.
j	Index for the D2D pairs.
l	Index for the D2D pair of interest, whose signal is the useful one.
k	Index for the cellular uplink users.
K	Number of frequency bands supported by both UAV and D2D communications.
W	Bandwidth of each of the multiple bands.
$\Phi_{d,i}$	Homogeneous PPP distribution for D2D users working in the i^{th} band.
$\Phi_{c,i}$	Homogeneous PPP distribution for the uplink cellular users working in the i^{th} band.
$\gamma_{d,l,i}$	SINR at the l^{th} D2D pair receiver working on the i^{th} band.
$P^r_{d,l,i}$	Power received at the l^{th} D2D pair receiver working in the i^{th} band.
$I^c_{d,l,i}$	Interference of the D2D pairs transmitters on the l^{th} D2D pair receiver in the i^{th} band.
I_u, i	Interference due to uplink users served by the UAV in the i^{th} band.
N_0	Additive white Gaussian noise.
$P^t_{d,i}$	Power transmitted by any D2D transmitter in the i^{th} band.
$R_{d,l,l}$	Distance between the transmitter and receiver of the l^{th} D2D pair.
$h_{l,l}$	Rayleigh fading coefficient of the link between the transmitter and receiver of the l^{th} D2D pair.
$h_{j,l}$	Rayleigh fading coefficient of the link between the j^{th} D2D pair transmitter and the l^{th} D2D pair receiver.
$R_{d,j,l}$	Distance between the j^{th} D2D pair transmitter and the l^{th} D2D pair receiver.
$P^r_{u,k,i}$	Power received at the UAV from the k^{th} cellular user on the i^{th} band.
$I_{d,i}$	Power of interference from all the D2D pairs received at the UAV on the i^{th} band.
$I^c_{u,k,i}$	Power of interference received at k^{th} user due to other cellular users working on the i^{th} band.
$\mathrm{P}_{\mathrm{LoS,k}}$	Probability of line-of-sight between the UAV and the k^{th} user.
$\mathrm{P}_{\mathrm{NLoS,k}}$	Probability of non-line-of-sight between the UAV and the k^{th} user.
$P^t_{u,i}$	Power transmitted by each cellular user on the i^{th} band.
α_d	Path-loss exponent of the links between D2D pairs.
α_u	Path-loss exponent for the links connected to the UAV.
θ_k	Elevation angle of the k^{th} user toward the UAV.
H	UAV altitude.
r_k	Distance between the k^{th} cellular user and the point of intersection of the three cells.
B & C	Constants for calculating the probability of LoS and they depend on the characteristics of the deployment environment.

$R_{d,j,l}$ refers to the distance between the receiver of the l^{th} D2D pair, and the the transmitter of the j^{th} D2D pair, $R_{d,l,l}$ denotes the distance between the transmitter and the receiver of the l^{th} D2D pair, and α_d is the path-loss exponent of the environment surrounding the D2D network.

The SINR expression for an uplink user k served by the UAV BS in the i^{th} band is:

$$\gamma_{u,k,i} = \frac{P^r_{u,k,i}}{I_{d,i} + I^c_{u,k,i} + N_0} \overset{(a)}{=} \frac{P^r_{u,k,i}}{I_{d,i} + N_0} \tag{4}$$

where $P^r_{u,k,i}$ denotes the power of the desired signal transmitted from k^{th} user to the UAV BS in the i^{th} band, $I_{d,i}$ refers to the power of the interference due to all the transmission of the D2D communications occur in the i^{th} band, and $I^c_{u,k,i}$ stands for the power of the transmissions from uplink users, excluding user k, operating on the same band as user k. The expression in (a) follows from the fact that, within each cell the UAV is communicating with the cellular users using orthogonal channels. The expression for $I_{d,i}$ is:

$$I_{d,i} = \sum_{j \in \Phi_{d,i}} P^t_{d,i} R^{-\alpha_d}_{u,j} h_{u,j} \tag{5}$$

The expressions for $P^r_{u,k,i}$, $I^c_{u,k,i}$ and $I_{u,i}$ can be easily defined based on the definition of the A2G channel model. According to [29], the A2G signals received at the ground receiver are composed of line-of-sight (LoS), strongly reflected non-LOS (NLoS), and multiple reflected components. These components are independent and according to [29] and [38], they could be involved through the consideration of probabilistic occurrence of each component. The probability of each of these components is a function of the environment parameters, elevation angle, height, and density of surrounding buildings. Typically, the A2G is modeled by considering a probabilistic superposition contribution of both the LoS and NLoS. By considering both the LoS and NLoS links between the UAV and any user, the signal power received at the UAV from user k on the i^{th} band could be expressed as [10]:

$$P^r_{u,k,i} = \left(\mathrm{P}_{\mathrm{LoS,k}} + \eta\, \mathrm{P}_{\mathrm{NLoS,k}}\right) P^t_{u,i} \left|R_{u,k,i}\right|^{-\alpha_u} \tag{6}$$

where $P^t_{u,i}$ is the uplink transmit power of any cellular user on band i, $\mathrm{P}_{\mathrm{LoS,k}}$ denotes the probability of occurrence of the LoS component for user k, $\mathrm{P}_{\mathrm{NLoS,k}}$ is the probability of occurrence of NLoS component of the link between the UAV and the k^{th} user; $\mathrm{P}_{\mathrm{NLoS,k}} = 1 - \mathrm{P}_{\mathrm{LoS,k}}$ for any user k, α_u is the pathloss exponent over the cellular user to UAV link, and η denotes an extra attenuation factor for the NLoS links. The probability of LoS for any user k is a function of the environment, density and height of surrounding buildings, the distance between the users and UAV, and the elevation angle between the user and UAV. Accordingly, it could be expressed as [10]:

$$\mathrm{P}_{\mathrm{LoS,k}} = \frac{1}{1 + C \exp\left(-B\left[\theta_k - C\right]\right)} \tag{7}$$

where C and B are constant values that depend on the characteristics of the deployment environment, and θ_k refers to the elevation angle associated with user k. If the altitude of the UAV is assumed to be H meters, then θ_k can be expressed as $\theta_k = \frac{180}{\pi} \times sin^{-1}\left(\frac{H}{|R_{u,k}|}\right)$, where $R_{u,k} = \sqrt{H^2 + r_k^2}$ with r_k denoting the distance between the intersection point of the three cells and user k. It is obvious from (7) that $\mathrm{P}_{\mathrm{LoS,k}}$ increases with increasing the elevation angle between the UAV and the k^{th}user.

III. ENERGY EFFICIENCY EVALUATION FOR MULTI-CELL MULTI-BAND STATIC UAV-ASSISTED NETWORK

The evaluation of the EE for D2D communication underlaying UAV depends on firstly evaluating the successful transmission probability as well as the average sum rate for both the D2D and uplink cellular users. The SINR-based successful transmission probabilities for the uplink cellular users and the D2D users are given by:

$$\mathrm{STP}_u(\gamma_{th,u}) = \Pr\left(\gamma_{u,k,i} \geq \gamma_{th,u}\right) \tag{8}$$

$$\mathrm{STP}_d(\gamma_{th,d}) = \Pr\left(\gamma_{d,l,i} \geq \gamma_{th,d}\right) \tag{9}$$

where $\mathrm{STP}_u(\cdot)$ denotes the successful transmission probability of the uplink cellular user, and $\mathrm{STP}_d(\cdot)$ represents the successful transmission probability of the D2D user. The symbols $\gamma_{th,u}$ and $\gamma_{th,d}$ represent the SINR threshold for the uplink cellular users and D2D users, respectively.

A. SUCCESSFUL TRANSMISSION PROBABILITY

One of the main performance metrics for evaluating uplink transmission strategies, specially in disaster times, is the successful transmission probability. It is worth noting that the successful transmission probability is an indication of the outage probability, namely *POT*, where the summation of the successful transmission and outage probabilities is equal to one, $STP + POT = 1$. Additionally, the successful transmission probability for uplink connection is analogous to the coverage probability for the downlink connection. In the following subsections, we evaluate the successful transmission probability for both the D2D and uplink cellular users in a scenario in which one UAV base station is hovering at an altitude H. Since we assume a uniform distribution of users in the three cells, placing the UAV at the point of intersection of the three cells[5] can achieve maximum successful transmission probability for the uplink cellular users [36].

1) SUCCESSFUL TRANSMISSION PROBABILITY FOR D2D USERS

Lemma 1: The successful transmission probability of the l^{th} pair D2D receiver in the i^{th} band located at distance $R_{d,l,l}$ from its pair transmitter, is given by:

$$\begin{aligned}&\mathrm{STP}_d(\gamma_{th,d})\\ &= \Pr(\gamma_{d,l,i} \geq \gamma_{th,d})\\ &= \exp\left(-\zeta_{c,i}\left(\lambda_{d,i}+\lambda_{c,i}\left(\frac{P^t_{u,i}}{P^t_{d,i}}\right)^{\frac{2}{\alpha_d}}\right) - \frac{\gamma_{th,d}R^{\alpha_d}_{d,l,l}\mathrm{N}_0}{P^t_{d,i}}\right),\end{aligned} \tag{10}$$

where $\gamma_{th,d}$ represents the SINR threshold of the D2D communication links, and

$$\zeta_{c,i} = \pi\gamma^{\frac{2}{\alpha_d}}_{th,d}R^2_{d,l,l}\Gamma\left(1+\frac{2}{\alpha_d}\right)\Gamma\left(1-\frac{2}{\alpha_d}\right). \tag{11}$$

[5]This is the central point of the whole service area which is also the center of the circle that touches each cell circle in only one point.

where for any positive integer z, $\Gamma(z)$ is the gamma function of z which is mathematically expressed as $\Gamma(z) = \int_0^\infty x^{z-1}e^{-x}dx$.

Proof: See Appendix A.

Lemma 1 shows the interaction between the network parameters and the successful transmission probability of a D2D communication receiver, and based on it, we can illustrate several key notes. First of all, as the threshold $\gamma_{th,d}$ increases, the condition $\gamma_{d,l,i} \geq \gamma_{th,d}$ becomes much difficult to be achieved, and accordingly the successful transmission probability will decrease. The density distributions of both the cellular users $\lambda_{c,i}$ and D2D users $\lambda_{d,i}$ change in inverse exponential way with the successful transmission probability. In other words, the successful transmission probability increases as the densities $\lambda_{c,i}$ and $\lambda_{d,i}$ becomes sparser due to the reduction in the interference power excreted at the D2D receiver. The interference power due to uplink cellular users increases as their transmission powers increase $P_{u,i}$, and the successful transmission probability decreases accordingly. Furthermore, the successful transmission probability could be increased through increasing the transmission powers of the D2D communications, $P^t_{d,i}$. Finally, the UAV parameters do not have any effect on the successful transmission probability of the D2D receiver in the uplink case where all the signals, including useful or inference signals, are transmitted using ordinary ground links and there is no involvement for the A2G links.

2) SUCCESSFUL TRANSMISSION PROBABILITY OF THE UAV

Lemma 2: The successful transmission probability for the flying UAV BS, when receiving a transmission from uplink cellular user k with coordinates (r, ϕ) in the i^{th} band, is given by:

$$\begin{aligned}STP_u\left(\gamma_{th,u}\right) &= \Pr\left(\gamma_{u,k,i} \geq \gamma_{th,u}\right)\\ &= \mathrm{P}_{\mathrm{LoS,k}}(r)\mathrm{I}\left(\frac{P^t_{u,i}r^{-\alpha_u} - \gamma_{th,u}N_0}{\gamma_{th,u}}\right)\\ &\quad + \mathrm{P}_{\mathrm{NLoS}}(r)\mathrm{I}\left(\frac{\eta P^t_{u,i}r^{-\alpha_u} - \gamma_{th,u}N_0}{\gamma_{th,u}}\right)\end{aligned} \tag{12}$$

where the function $\mathrm{I}(\cdot)$ is defined as:

$$\begin{aligned}I(A) &= \left(1 - \frac{2\pi\lambda_{d,i}\Gamma\left(1+\frac{2}{\alpha_u}\right)}{\alpha_u - 2}\left(\frac{A}{P^t_{d,i}}\right)^{-\frac{2}{\alpha_u}}\right)\\ &\quad \times \exp\left(-\pi\lambda_{d,i}\left(\frac{A}{P^t_{d,i}}\right)^{\frac{-2}{\alpha_u}}\Gamma\left(1+\frac{2}{\alpha_u}\right)\right)\end{aligned} \tag{13}$$

Proof: See Appendix B.

It is obvious from **Lemma 2** that the parameters of the UAV flying BS and its channels with different users have a critical effect on the successful transmission probability at the UAV $STP_u(\gamma_{th,u})$. In order to illustrate the effect of the number of D2D pairs on $STP_u(\gamma_{th,u})$, let $\lambda_{d,i} \to 0$, which means that the number of D2D pairs tends to zero and consequently no

interference is encountered by D2D pairs. The interference originated due to an increase in D2D pairs will grow to infinity and the exponential term in (13) equals zero, and hence the transmission eventually failed since $STP_u(\gamma_{th,u}) = 0$. The effect of UAV and its channels' parameters included in both $\mathrm{P_{LoS,k}}$ and $\mathrm{P_{NLoS,k}}$. From (7), (12), and (13), we can note that the altitude of the UAV, H, has a direct effect on the LoS probability $\mathrm{P_{LoS}}$. Specifically, as the UAV altitude increases, this consequently improves $\mathrm{P_{LoS}}$. However, increasing H and consequently $R_{u,k}$ leads to decreasing $I(A)$ in (13) and consequently degrades the successful transmission probability STP_u. Based on such trade-off between H and $\mathrm{STP_u}$, the altitude needs a careful adjustment in order to achieve the maximum successful transmission probability.

B. AVERAGE SUM RATE AND ENERGY EFFICIENCY

Let $C_{d,i}$ be the average sum-rate of D2D communication pair in the i^{th} band. With the known SINR threshold $\gamma_{th,d}$, if follows from [10] and [35] that the average achievable sum-rate for an D2D users pair is given as:

$$C_{d,i} = W_i \log_2\left(1+\gamma_{th,d}\right) \Pr\left(\gamma_{d,l,i} \geq \gamma_{th,d}\right) \tag{14}$$

where W_i is the transmission bandwidth of the i^{th} band. According to **Lemma 1**, (14) can be rewritten as

$$\begin{aligned} C_{d,i} &= W_i \log_2\left(1+\gamma_{th,d}\right) \\ &\quad \times \exp\left(-\zeta_{c,i}\left(\lambda_{d,i}+\lambda_{c,i}\left(\frac{P^t_{u,i}}{P^t_{d,i}}\right)^{\frac{2}{\alpha_d}}\right) - \frac{\gamma_{th,d} R^{\alpha_d}_{d,l,l} \mathrm{N_0}}{P^t_{d,i}}\right). \end{aligned} \tag{15}$$

Similarly, the average sum-rate of an uplink cellular user through the UAV in the i^{th} band, namely, $C_{u,i}$, is given as

$$\begin{aligned} C_{u,i} &= W_i \log_2\left(1+\gamma_{th,u}\right) \Pr\left(\gamma_{u,k,i} \geq \gamma_{th,u}\right) \\ &= W_i \log_2\left(1+\gamma_{th,u}\right) \\ &\quad \times \left(\mathrm{P_{LoS,k}}(r)\mathrm{I}\left(\frac{P^t_{u,i} r^{-\alpha_u} - \gamma_{th,u} N_0}{\gamma_{th,u}}\right)\right. \\ &\quad \left. + \mathrm{P_{NLoS}}(r)\mathrm{I}\left(\frac{\eta P^t_{u,i} r^{-\alpha_u} - \gamma_{th,u} N_0}{\gamma_{th,u}}\right)\right). \end{aligned} \tag{16}$$

where the function $I(\cdot)$ is defined in (13). Accordingly, the sum-rates of the D2D and uplink cellular communications within the i^{th} band could be expressed, respectively, as[6]:

$$\begin{aligned} \mathbb{R}_{d,i} &= \pi (2R_c)^2 \lambda_{d,i} C_{d,i} \\ &= 4\pi R_c^2 \lambda_{d,i} W_i \log_2\left(1+\gamma_{th,d}\right) \\ &\quad \times \exp\left(-\zeta_{c,i}\left(\lambda_{d,i}+\lambda_{c,i}\left(\frac{P^t_{u,i}}{P^t_{d,i}}\right)^{\frac{2}{\alpha_d}}\right) - \frac{\gamma_{th,d} R^{\alpha_d}_{d,l,l} \mathrm{N_0}}{P^t_{d,i}}\right), \end{aligned} \tag{17}$$

[6]The numbers of D2D users and uplink cellular users in the whole cellular system (circle with radius $2R_c$) are $4\pi R_c^2 \lambda_{d,i}$ and $4\pi R_c^2 \lambda_{c,i}$, respectively.

and

$$\begin{aligned} \mathbb{R}_{u,i} &= \lambda_{u,i} \int_0^{2R_c} C_{u,i}\, dr \\ &= \lambda_{u,i} W_i \log_2\left(1+\gamma_{th,u}\right) \\ &\quad \times \int_0^{2R_c} \left(\mathrm{P_{LoS,k}}(r)\mathrm{I}\left(\frac{P^t_{u,i} r^{-\alpha_u} - \gamma_{th,u} N_0}{\gamma_{th,u}}\right)\right. \\ &\quad \left. + \mathrm{P_{NLoS}}(r)\mathrm{I}\left(\frac{\eta P^t_{u,i} r^{-\alpha_u} - \gamma_{th,u} N_0}{\gamma_{th,u}}\right)\right) dr. \end{aligned} \tag{18}$$

In disaster recovery scenarios for D2D communications undelaying an UAV, it is of great importance to consider the EE for the D2D and uplink cellular communications through the UAV. Firstly, the EE for D2D communication on band i could be defined as the average sum-rate on band i divided by the total power consumption on that band [35]. Based on the principles of stochastic geometry, the consumed power by users working in band i can be calculated as $\lambda_{d,i} \cdot P^t_{d,i}$. Accordingly, the EE of the D2D communications in band i, when it is underlaid by UAV, could be calculated as

$$\begin{aligned} &\mathbb{EE}_{d,i} \\ &= \frac{\mathbb{R}_{d,i}}{(4\pi R_c^2)(\lambda_{d,i}) P^t_{d,i}} = \frac{C_{d,i}}{P^t_{d,i}} \\ &= \frac{W_i}{P^t_{d,i}} \log_2\left(1+\gamma_{th,d}\right) \\ &\quad \times \exp\left(-\zeta_{c,i}\left(\lambda_{d,i}+\lambda_{c,i}\left(\frac{P^t_{u,i}}{P^t_{d,i}}\right)^{\frac{2}{\alpha_d}}\right) - \frac{\gamma_{th,d} R^{\alpha_d}_{d,l,l} \mathrm{N_0}}{P^t_{d,i}}\right). \end{aligned} \tag{19}$$

By utilizing similar manipulations, the EE of the uplink cellular users' communications through the UAV could be expressed as

$$\begin{aligned} \mathbb{EE}_{u,i} &= \frac{\mathbb{R}_{u,i}}{(4\pi R_c^2)(\lambda_{u,i}) P^t_{u,i}} = \frac{C_{u,i}}{(4\pi R_c^2)(P^t_{u,i})} \\ &= \frac{W_i}{(4\pi R_c^2)(P^t_{u,i})} \log_2\left(1+\gamma_{th,u}\right) \\ &\quad \times \int_0^{2R_c} \left(\mathrm{P_{LoS,k}}(r)\mathrm{I}\left(\frac{P^t_{u,i} r^{-\alpha_u} - \gamma_{th,u} N_0}{\gamma_{th,u}}\right)\right. \\ &\quad \left. + \mathrm{P_{NLoS}}(r)\mathrm{I}\left(\frac{\eta P_{u,i} r^{-\alpha_u} - \gamma_{th,u} N_0}{\gamma_{th,u}}\right)\right) dr. \end{aligned} \tag{20}$$

Based on (19) and (20), the total EE of the whole network on all bands, which is the ratio of the total sum-rate and the total power consumption of both the D2D and uplink cellular communications through the UAV [39], is computed as

$$\mathbb{EE}_{tot} = \frac{\sum_{i=1}^{K}\left(\mathbb{R}_{d,i}+\mathbb{R}_{u,i}\right)}{(4\pi R_c^2)\sum_{i=1}^{K}\left(\lambda_{d,i} P^t_{d,i} + \lambda_{c,i} P^t_{u,i}\right)} \tag{21}$$

It follows from (10), (12), (13), (19) and (20) that the EE depends on the users density, whether D2D or uplink cellular users, exactly as the successful transmission probability does.

TABLE 2. Simulation parameters.

Parameter	Value
K	5
$P^t_{u,i}$	300, 350, 400 mW
$P^t_{d,i}$	100, 150, 200 mW
N_0	-120 dBm
W_i	5 MHz
α_d	4
α_u	2
η	20 dB
B & C	0.136 & 11.95
$\gamma_{th,d}$	0 dB
$\gamma_{th,u}$	0 dB

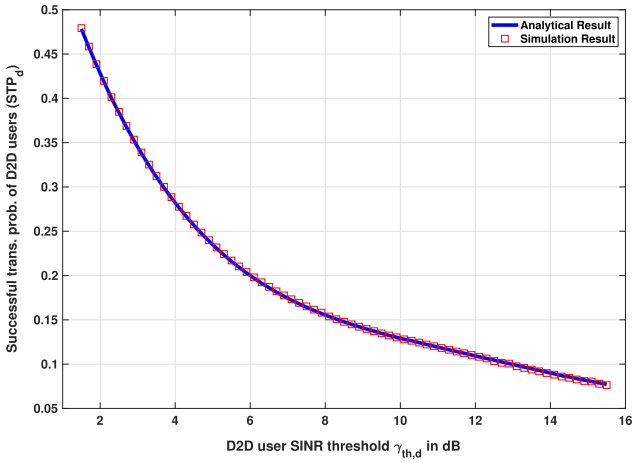

FIGURE 2. D2D successful transmission probability vs. their SINR Threshold.

IV. SIMULATION RESULTS

In this section, we study the EE performance of both the UAV and D2D communications, when they coexist in post-disaster scenarios, using both simulations and mathematical expressions derived in Section III. Based on the simulation parameters listed in Table 2, we first prove the complete matching of the successful transmission probabilities between the simulations and analytical results obtained using the mathematical expressions in Lemmas 1 and 2. Then, we investigate the impact of different network parameters, i.e., D2D density $\lambda_{d,i}$, uplink users density $\lambda_{u,i}$, UAV altitude H, and SINR thresholds $\{\gamma_{th,d}, \gamma_{th,u}\}$, on the EE of the D2D communication underlaying UAV post-disaster network.

Figs 2 and 3 show the perfect match between the simulation and analytical results in terms of the successful transmission probability of both D2D users and UAV-connected uplink users. Fig. 2 shows the variation of the successful transmission probability for D2D users versus the SINR threshold of D2D users. On the other hand, Fig. 3 displays the variation of the successful transmission probability for UAV-connected uplink users versus the SINR threshold of the UAV-connected uplink user. It is clear from Figs. 2 and 3 that the successful transmission probability for D2D and UAV-connected uplink users decreases as the densities of users increase.

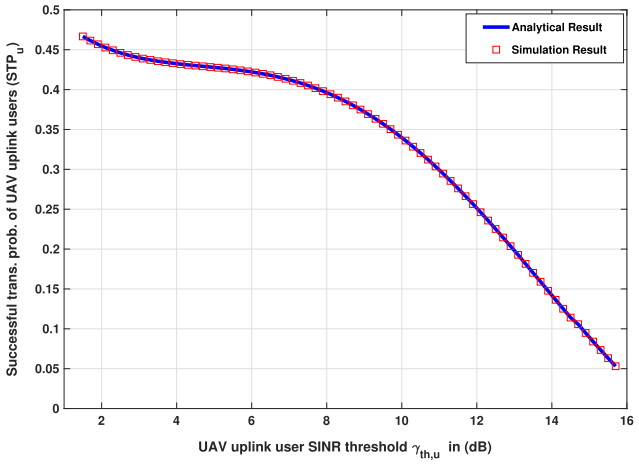

FIGURE 3. UAV-connected uplink users' successful transmission probability vs. their SINR Threshold.

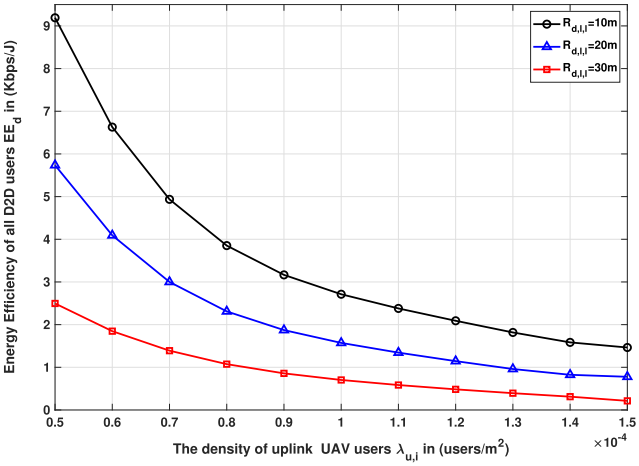

FIGURE 4. Accumulated energy efficiency of D2D users EE_d vs UAV-connected uplink user density $\lambda_{u,i}$.

Fig. 4 illustrates the impact of the density of UAV-connected uplink users on the accumulated EE of all D2D users, namely EE_d, at different values for the distance between D2D pairs, i.e., $R_{d,l,l} = \{10, 20, 30\}$ m. In this scenario, we use $P^t_{u,i} = 300$ milliWatt (mW), $P^t_{d,i} = 100$ mW, and $\lambda_{d,i} = 10^{-4}$users/m^2. It can be clearly noticed that the accumulated EE of the D2D pairs decreases with the increase of the density of the UAV-connected uplink users. This is due to the growing amount of D2D power consumed to coordinate the interference generated as a consequence of the increased density of UAV-connected users, which in turn results in the decrease of their accumulated EE. It can also be noticed that, as the distance between the D2D pairs increases, the accumulated EE of D2D users will accordingly decreases. This can be explained by exploiting the effect of channel fading on the D2D signal transmission. In other words, the effect of channel fading becomes more serious as the transmission distance between the D2D pairs increases, which in turn leads to a decrease in the average sum-rate and accordingly the EE of the D2D users in the network.

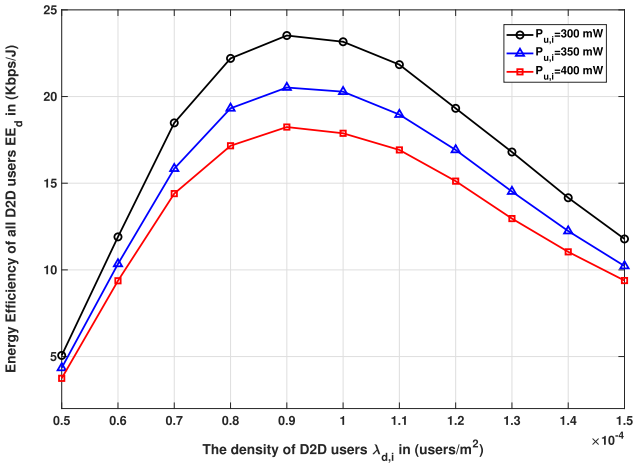

FIGURE 5. Accumulated energy efficiency of D2D users EE_d vs D2D users density $\lambda_{d,i}$.

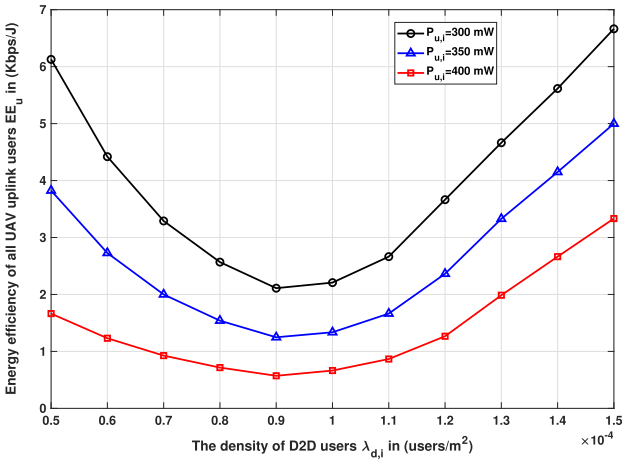

FIGURE 7. Accumulated EE of UAV-connected users EE_u vs D2D users density $\lambda_{d,i}$ at different values of uplink user transmit power $P^t_{u,i}$.

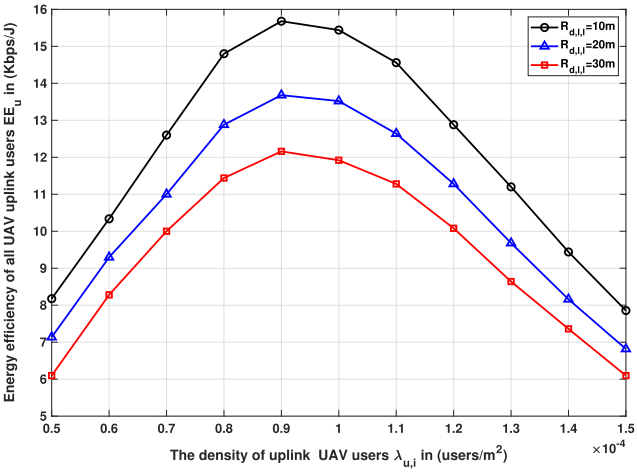

FIGURE 6. Accumulated EE of UAV-connected users EE_u vs UAV-connected uplink user density $\lambda_{u,i}$ at different D2D pair distance.

Fig. 5 exploits the variation of the accumulated D2D users' EE, i.e., EE_d, with both D2D users density and the transmission power of UAV-connected uplink users. It is assumed here that $P^t_{d,i} = 100\,\text{mW}$ and $\lambda_{c,i} = 2 \times 10^{-5}\text{users/m}^2$. It is noticed that the EE grows at first with the increase of D2D users density, and then declines with more increase of the D2D users density. First, when the D2D users density is relatively small, the interference resulted from sharing the same spectrum band is relatively small compared to the useful signal transferred on that band and consequently the EE increases with increasing the D2D users density. After a certain level of D2D users density, the EE begins to decline due to the severe increase of the excreted interference and consequently more D2D transmission power are consumed to coordinate the interference and consequently the EE of D2D users decreases with more increase of D2D users' density.

Figs. 6 and 7 investigate the variation of the accumulated EE of UAV-connected users with both uplink and D2D users densities, D2D pairs distance, and uplink users transmit powers. In Fig. 6, it is obvious that the EE of UAV-based connections first increases with the increase of the uplink users density and then declines when their generated interference crosses a specific limit at which more power is consumed to coordinate such interference and accordingly both the sum-rate and EE decrease. The inflection points of the curves represent the optimum uplink users densities at different values of the D2D pair distance. Moreover, it is seen from Fig. 6 that the EE decreases as the D2D pair distance increases. Similar to the aforementioned discussions on Fig. 4, Fig. 7 shows that the EE of uplink UAV-connected users is generally decreases with the increase of the transmission powers $P^t_{u,i}$ due to the interference they exert on each others and on D2D receivers. Since the transmission powers of the UAV-connected user is three times of more than that of its D2D counterparts, the UAV communications are still able to achieve much more EE as the D2D users densities increase.

Figs. 8 and 9 highlight the performance of the whole network EE which is the summation of both the D2D and uplink users EE. Fig. 8 is the summation of the results given in Figs. 4 and 6. Also Fig. 9 is the summation of the results given in Figs. 5 and 7. The EE of the whole network follows the same behavior as that of both D2D and UAV-based communications.

Fig. 10 illustrates the total EE (Kbps/Joule) versus the UAV uplink SINR threshold ($\gamma_{th,u}$). In Fig. 10, we use $\lambda_{d,i} = 10^{-5}$, $H = 650\text{m}$, and two different values of D2D users' densities. As we discussed in **Section** III, the total EE depends on the successful transmission probabilities $\text{STP}_d(\gamma_{th,d})$ and $\text{STP}_u(\gamma_{th,u})$. Based on (17)-(21), it is noticed that behind the dependence of the total EE on the successful transmission probabilities, which are functions of their corresponding SINR thresholds, it depends also on an increasing logarithmic functions of the SINR thresholds, namely, $\log_2(1+\gamma_{th,d})$ and $\log_2(1+\gamma_{th,u})$. It is obvious that, as the SINR threshold becomes very high, it will be very difficult for the received SINR to exceed such thresholds, and accordingly the successful transmission probabilities for the

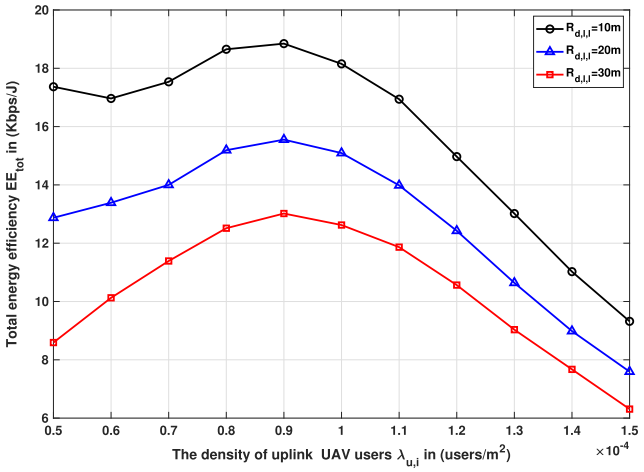

FIGURE 8. Total EE vs. uplink UAV-connected users' density $\lambda_{u,i}$ at different D2D pair distance values.

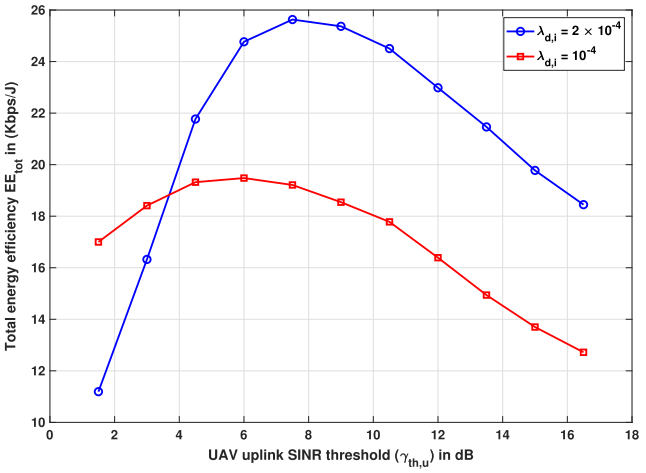

FIGURE 10. Total EE vs. UAV uplink SINR threshold ($\gamma_{th,u}$) for different D2D users density.

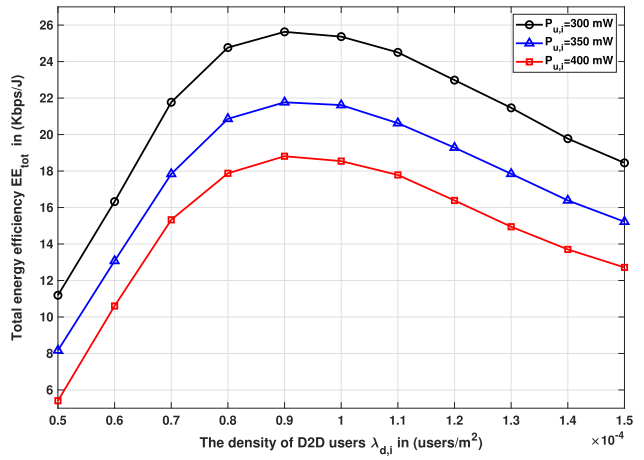

FIGURE 9. Total EE vs. D2D users' density $\lambda_{d,i}$ at different transmission power levels.

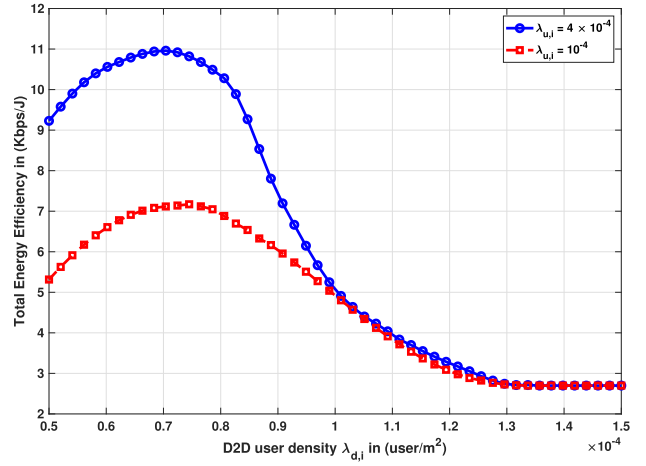

FIGURE 11. Total EE vs. D2D user density ($\lambda_{d,i}$) for different uplink users density.

D2D and UAV-connected uplink users approach zero. At the same time, $\log_2(1+\gamma_{th,d})$ and $\log_2(1+\gamma_{th,u})$ increase as the thresholds $\gamma_{th,d}$ and $\gamma_{th,u}$ increase. For $\gamma_{th,u} \to 0$ and $\gamma_{th,d} \to 0$, the $\log_2(1+\gamma_{th,d}) \to 0$ and $\log_2(1+\gamma_{th,u}) \to 0$, and accordingly $\text{STP}_\text{u} \to 1$, $\text{STP}_\text{d} \to 1$, this in turn means that the total EE, $\mathbb{EE}_{tot}$, tends zero.

Fig. 11 shows the impact of the D2D users' density on the total EE of the network. It is clear that decreasing $\lambda_{d,i}$ leads to lower interference suffered due to spectrum sharing, and accordingly lower power consumed to coordinate such interference, which in turn results in high EE. It is observed from Fig. 11 that, as the UAV-connected uplink users density $\lambda_{u,i}$ increases, the optimal D2D user density $\lambda_{d,i}$ that maximizes the EE decreases. The cause behind that phenomena is that, as $\lambda_{u,i}$ increases, the sum-rate and accordingly the EE will increase accordingly. In order to obtain such an increase in EE and sum-rate, the interference exerted due to the existence of D2D users should be decreased, and finally it turns out that the optimal $\lambda_{d,i}$ becomes smaller as $\lambda_{u,i}$ increases.

Fig. 12 displays the optimal UAV altitude that maximizes the successful transmission probability versus the D2D users' density. It is clear from Fig. 12 that the optimum UAV altitude is independent of the distance between D2D transmitter-receiver pair $R_{d,l,l}$. This is due to the fact that $R_{d,l,l}$ does not affect the amount of interference generated by D2D users at the UAV. It is also shown from Fig. 12 that the optimum UAV altitude decreases as the number of D2D users' density increases. The reason behind such phenomena is that increasing the D2D users' density will result in an increased interference on the UAV BS, which forces the UAV to reduce its altitude to improve the received SINR at the UAV BS and accordingly improves both the sum-rate and EE.

Fig. 13 shows the variation of the total EE with the UAV altitude for different values of D2D Tx-Rx pair distance. The optimum UAV altitudes corresponding to the maximum total EE are 320m, 360m, 400m for D2D transmitter-receiver pair distances of 20m, 30m, and 40m, respectively. It is clear from Fig. 13 that, the smaller the D2D transmitter-receiver pair distance, the higher the resulting total EE. Moreover, at the

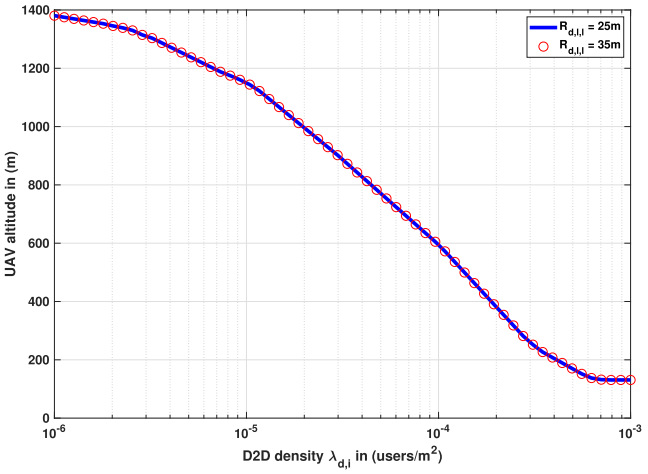

FIGURE 12. Optimum altitude of the UAV BS vs D2D users' density.

UAV altitudes of more than 1400m, the successful transmission probability of UAV-connected uplink users approaches zero and accordingly the whole contributions of the EE and sum-rate are due to D2D users, and as the UAV altitude becomes higher than 1400m, the D2D contributions increase due to the reduction of the interference generated by the UAV communications as a result of lacking the UAV coverage. For the UAV altitude in the range $400m < H < 1400m$ with different values of $R_{d,l,l}$, the successful transmission probability, average sum-rate, and EE of uplink users decreases with the increase of UAV altitude. Moreover, increasing the UAV altitude may make the UAV-connected users to raise their transmit powers into order for the uplink transmissions to be received safely at the UAV BS, which in turn leads to a subsequent increase in the amount of interference exerted on D2D users and consequently decreases their EE contributions.

V. CONCLUSION

In this paper, we have proposed a network planning strategy for post-disaster situations by employing a flying UAV BS to serve an area which originally covered by three terrestrial BSs. Moreover, we have assumed that some users in the network are involved in D2D communications. We have investigated the performance of the uplink of the UAV-assisted network that is underlaid with some D2D communications. We have derived tractable expressions for the successful transmission probability, the average sum-rate, and the EEs of both the D2D and the UAV-connected uplink users. Finally, we have studied the trade-off between different network parameters and have given some insights about the optimum UAV altitude that achieves the maximum EE which is the most critical performance metric in disaster situations.

APPENDIX A
PROOF OF LEMMA 1

This appendix derives the expression of the successful transmission probability for the D2D user with interference of UAV-connected uplink users. The successful transmission probability is computed as

$$\begin{aligned}
&\Pr\left(\gamma_{d,l,i} \geq \gamma_{th,d}\right) \\
&= \Pr\left(\frac{P^r_{d,l,i}}{I^c_{d,l,i} + I_{u,i} + \mathrm{N}_0} \geq \gamma_{th,d}\right) \\
&= \Pr\left(\frac{P^t_{d,i} R^{-\alpha_d}_{d,l,l} h_{l,l}}{I^c_{d,l,i} + I_{u,i} + \mathrm{N}_0} \geq \gamma_{th,d}\right) \\
&\overset{(a)}{=} \mathbb{E}_{I^c_{d,l,i}}\left[\exp\left(\frac{-\gamma_{th,d} R^{\alpha_d}_{d,l,l} I^c_{d,l,i}}{P^t_{d,i}}\right)\right] \\
&\quad \times \mathbb{E}_{I_{u,i}}\left[\exp\left(\frac{-\gamma_{th,d} R^{\alpha_d}_{d,l,l} I_{u,i}}{P^t_{d,i}}\right)\right] \\
&\quad \times \exp\left(\frac{-\gamma_{th,d} R^{\alpha_d}_{d2d,l,l} \mathrm{N}_0}{P^t_{d,i}}\right) \\
&\overset{(b)}{=} \mathbb{E}_{I^c_{d,l,i}}\left[\prod_{j\in\Phi_{d,i}} \exp\left(-\gamma_{th,d} R^{\alpha_d}_{d,l,l} R^{-\alpha_d}_{d,j,l} h_{j,l}\right)\right] \\
&\quad \times \mathbb{E}_{I_{u,i}}\left[\prod_{k\in\Phi_{c,i}} \exp\left(-\gamma_{th,d} R^{\alpha_d}_{d,l,l}\left(\frac{P^t_{u,i}}{P^t_{d,i}}\right) R^{-\alpha_d}_{d,k,l} h_{kl}\right)\right] \\
&\quad \times \exp\left(\frac{-\gamma_{th,d} R^{\alpha_d}_{d,l,l} \mathrm{N}_0}{P^t_{d,i}}\right), \qquad (22)
\end{aligned}$$

where (a) depends on the characteristics of exponential distribution and Rayleigh fading assumption, and (b) results from the fact that different interference components are independent. By assuming that the D2D receiver is at location (r, ϕ), and its pair transmitter is located at a distance $R_{d,l,l}$ away from it, based on the stochastic geometry principles, we can verify

$$\begin{aligned}
&\mathbb{E}_{I^c_{d,l,i}}\left[\prod_{j\in\Phi_{d,i}} \exp\left(-\gamma_{th,d} R^{\alpha_d}_{d,l,l} R^{-\alpha_d}_{d,j,l} h_{j,l}\right)\right] \\
&= \mathcal{L}_{I^c_{d,l,i}(h_{j,l})}\left(\gamma_{th,d} R^{\alpha_d}_{d,l,l}\right) \\
&= \exp\left[-\lambda_{d,i}\int_0^\infty \mathbb{E}\left(h_{j,l}\right)\left[1 - e^{\left(-\gamma_{th,d} R^{\alpha_d}_{d,l,l} r^{-\alpha_d}\right)}\right] dr\right] \\
&= \exp\left[-\lambda_{d,i}\pi \gamma^{\frac{2}{\alpha_d}}_{th,d} R^2_{d,l,l} \Gamma\left(1 + \frac{2}{\alpha_d}\right)\Gamma\left(1 - \frac{2}{\alpha_d}\right)\right] \qquad (23)
\end{aligned}$$

Similarly

$$\begin{aligned}
&\mathbb{E}_{I_{u,i}}\left[\prod_{k\in\Phi_{c,i}} \exp\left(-\gamma_{th,d} R^{\alpha_d}_{d,l,l}\left(\frac{P^t_{u,i}}{P^t_{d,i}}\right) R^{-\alpha_d}_{d,k,l} h_{k,l}\right)\right] \\
&= \mathcal{L}_{I_{u,i}(h_{k,l})}\left(\gamma_{th,d} R^{\alpha_d}_{d,l,l}\right) \\
&= \exp\left[-\lambda_{c,i}\left(\frac{P^t_{u,i}}{P^t_{d,i}}\right)^{\frac{2}{\alpha_d}} \pi \gamma^{\frac{2}{\alpha_d}}_{th,d} R^2_{d,l,l} \Gamma\left(1 + \frac{2}{\alpha_d}\right)\Gamma\left(1 - \frac{2}{\alpha_d}\right)\right] \qquad (24)
\end{aligned}$$

By taking into consideration the results obtained in (22)-(24), we can directly obtain the results mentioned in **Lemma** 1.

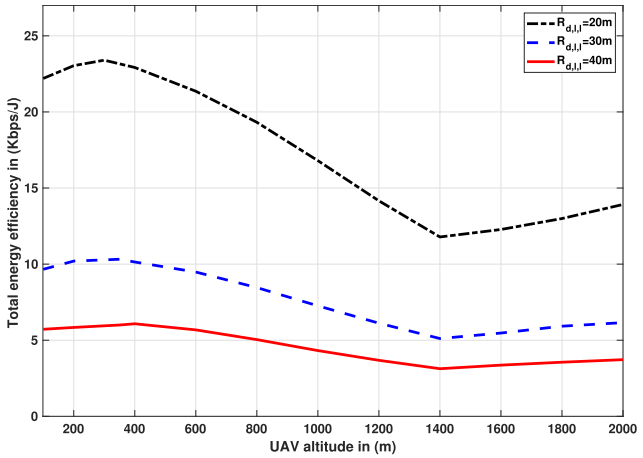

FIGURE 13. Total EE of the network vs the altitude of the UAV BS for different values of D2D Tx-Rx pair distance.

APPENDIX B
PROOF OF LEMMA 2

This appendix calculates the expression of the successful transmission probability for uplink cellular user who tries to connect to the UAV BS with interference from D2D users/transmissions on the i^{th} band. The successful transmission probability for an uplink cellular user at location (r, ϕ) is given by

$$\begin{aligned} STP_u\left(\gamma_{th,u}\right) &= \Pr\left(\gamma_{u,k,i} \geq \gamma_{th,u}\right) \\ &= \Pr\left(\frac{P^r_{u,k,i}}{I_{d,i}+\mathrm{N}_0} \geq \gamma_{th,u}\right) \\ &= \mathrm{P}_{\mathrm{LoS}}(r)\Pr\left(\frac{P^t_{u,i}\, r^{-\alpha_u}}{I_{d,i}+\mathrm{N}_0} \geq \gamma_{th,u}\right) \\ &\quad + \mathrm{P}_{\mathrm{NLoS}}(r)\Pr\left(\frac{\eta\, P^t_{u,i}\, r^{-\alpha_v}}{I_{d,i}+\mathrm{N}_0} \geq \gamma_{th,u}\right) \\ &= \mathrm{P}_{\mathrm{LoS}}(r)\Pr\left(I_{d,i} \leq \frac{P_{u,i}\, r^{-\alpha_u} - \gamma_{th,u}\,\mathrm{N}_0}{\gamma_{th,u}}\right) \\ &\quad + \mathrm{P}_{\mathrm{NLoS}}(r)\Pr\left(I_{d,i} \leq \frac{\eta\, P_{u,i}\, r^{-\alpha_u} - \gamma_{th,u}\,\mathrm{N}_0}{\gamma_{th,u}}\right) \end{aligned} \tag{25}$$

According to [23], [37], [38], the cumulative distribution function (CDF) of the interference, generated from the D2D users, has no closed-form solution. In order to determine $STP_u(\gamma_{th,u})$, we should first obtain an expression for the probability that the power of the D2D users interference is less than or equal a specific threshold, namely, $\Pr(I_{d,i} \leq A)$, where A is the threshold for deriving the CDF of the D2D users interference. Following the same way as in [23], suppose that the D2D transmitters which generate the interference are divided into two subsets, namely,

$$\begin{aligned} \Phi_1 &= \left\{\Phi_{d,i} | P^t_{d,i} R^{-\alpha_d}_{d,l,l} h_{l,l} \geq A\right\} \\ \Phi_2 &= \Phi_{d,i} - \Phi_1 \end{aligned} \tag{26}$$

Accordingly, the interference powers of the two subsets Φ_1 and Φ_2 can be referred to as I_{d,Φ_1}, and I_{d,Φ_2} respectively. The probability is calculated as

$$\begin{aligned} \Pr\left(I_{d,i} \leq A\right) &= \Pr\left(I_{d,\Phi_1} + I_{d,\Phi_2} \leq A\right) \\ &\leq \Pr\left(I_{d,\Phi_1} \leq A\right) \end{aligned} \tag{27}$$

We can consider the event that the interference power is less than the threshold equivalent to the event that $\Phi_1 = 0$. Mathematically, this can be written as

$$\begin{aligned} \Pr\left(I_{d,\Phi_1} \leq A\right) &\equiv \Pr\left(\Phi_1 = 0\right) \\ &= \mathbb{E}\left[\prod_{\Phi_{d,i}} \Pr\left(P^t_{d,i} R^{-\alpha_d}_{d,l,l} h_{l,l} \leq A\right)\right] \\ &= \mathbb{E}\left[\prod_{\Phi_{d,i}} \Pr\left(h_{l,l} \leq \frac{R^{\alpha_d}_{d,l,l} A}{P^t_{d,i}}\right)\right] \\ &\overset{(a)}{=} \mathbb{E}\left[\prod_{\Phi_{d,i}} \left(1 - \exp\left(\frac{-A R^{\alpha_d}_{d,l,l}}{P^t_{d,i}}\right)\right)\right] \\ &\overset{(b)}{=} \exp\left(-\lambda_{d,i} \int_0^\infty \frac{-A R^{\alpha_d}_{d,l,l}}{P^t_{d,i}} r dr\right) \\ &= \exp\left(-\pi \lambda_{d,i} \left(\frac{A}{P^t_{d,i}}\right)^{-\frac{2}{\alpha_d}} \Gamma\left(1+\frac{2}{\alpha_d}\right)\right) \end{aligned} \tag{28}$$

Note that (a) and (b) follow from the properties of Rayleigh fading channels and the probability generating function of the PPP [37], respectively. Based on (27), the CDF of the D2D interference can be derived as

$$\begin{aligned} &\Pr\left(I_{d,i} \leq A\right) \\ &\quad = 1 - \Pr\left(I_{d,i} \geq A\right) \\ &\quad = 1 - \Big[\Pr\left(I_{d,i} \geq A | I_{d,\Phi_1} \geq A\right)\Pr\left(I_{d,\Phi_1} \geq A\right) \\ &\qquad + \Pr\left(I_{d,i} \geq A | I_{d,\Phi_1} \leq A\right)\Pr\left(I_{d,\Phi_1} \leq A\right)\Big] \end{aligned} \tag{29}$$

Since $I_{d,i} \geq A$ guarantees $I_{d,\Phi_1} \geq A$. As a result, $\Pr\left(I_{d,i} \geq A | I_{d,\Phi_1} \geq A\right) = 1$. Then, (29) can be simplified as

$$\begin{aligned} &\Pr\left(I_{d,i} \leq A\right) \\ &\quad = 1 - \Big[\Pr\left(I_{d,\Phi_1} \geq A\right) \\ &\qquad + \Pr\left(I_{d,i} \geq A | I_{d,\Phi_1} \leq A\right)\Pr\left(I_{d,\Phi_1} \leq A\right)\Big] \\ &\quad = 1 - \Big[1 - \Pr\left(\Phi_1 = 0\right) \\ &\qquad + \Pr\left(I_{d2d,i} \geq A | \Phi_1 = 0\right)\Pr\left(\Phi_1 = 0\right)\Big] \\ &\quad = \Pr\left(\Phi_1 = 0\right)\Big[1 - \Pr\left(I_{d,i} \geq A | \Phi_1 = 0\right)\Big] \end{aligned} \tag{30}$$

Based on the Markov's inequality, we could attain

$$\begin{aligned} &\Pr\left(I_{d,i} \geq A | \Phi_1 = 0\right) \\ &\quad \leq \frac{\mathbb{E}\left(I_{d,i} \geq A | \Phi_1 = 0\right)}{A} \end{aligned}$$

$$
\begin{aligned}
&= \frac{1}{A}\mathbb{E}\left[\sum_{\Phi_{d,i}} P^t_{d,i} R^{-\alpha_d}_{d,l,l} h_{l,l} \mathbb{1}\left(P^t_{d,i} R^{-\alpha_d}_{d,l,l} h_{l,l} \leq A\right)\right] \\
&= \frac{1}{A}\mathbb{E}_{R_{d,l,l}}\Bigg[\sum_{\Phi_{d,i}} P^t_{d,i} R^{-\alpha_d}_{d,l,l} \\
&\quad \times \mathbb{E}_{h_{l,l}}\left(h_{l,l}\mathbb{1}\left(P^t_{d,i} R^{-\alpha_d}_{d,ll} h_{l,l} \leq A\right)\right)\Bigg] \\
&= \frac{1}{A}\mathbb{E}_{R_{d,l,l}}\left[\sum_{\Phi_{d,i}} P^t_{d,i} R^{-\alpha_d}_{d,l,l} \times \left(\int_0^{\frac{AR^{\alpha_d}_{d,l,l}}{P^t_{d,i}}} h e^{-h} dh\right)\right] \\
&= \frac{2\pi\lambda_{d,i} P^t_{d,i}}{A}\int_0^{\infty} r^{-\alpha_d}\left(\int_0^{\frac{Ar^{\alpha_d}}{P^t_{d,i}}} h e^{-h} dh\right) r dr \\
&= \frac{2\pi\lambda_{d,i}\Gamma\left(1+\frac{2}{\alpha_d}\right)}{\alpha_d - 2}\left(\frac{A}{P^t_{d,i}}\right)^{\frac{-2}{\alpha_d}} \qquad (31)
\end{aligned}
$$

Substituting (31) into (30), yields

$$
\begin{aligned}
&\Pr\left(I_{d,i} \leq A\right) \\
&\quad = \Pr\left(\Phi_1 = 0\right)\left[1 - \frac{2\pi\lambda_{d,i}\Gamma\left(1+\frac{2}{\alpha_d}\right)}{\alpha_d - 2}\left(\frac{A}{P^t_{d,i}}\right)^{\frac{-2}{\alpha_d}}\right] \qquad (32)
\end{aligned}
$$

Inserting (28) and (32) into (25) completes the proof of **Lemma** 2.

REFERENCES

[1] S. Hayat, E. Yanmaz, and R. Muzaffar, "Survey on unmanned aerial vehicle networks for civil applications: A communications viewpoint," *IEEE Commun. Surveys Tuts.*, vol. 18, no. 4, pp. 2624–2661, 4th Quart., 2016.

[2] Y. Zeng, R. Zhang, and T. J. Lim, "Wireless communications with unmanned aerial vehicles: Opportunities and challenges," *IEEE Commun. Mag.*, vol. 54, no. 5, pp. 36–42, May 2016.

[3] J. Zhao, F. Gao, Q. Wu, S. Jin, Y. Wu, and W. Jia, "Beam tracking for UAV mounted SatCom on-the-move with massive antenna array," *IEEE J. Sel. Areas Commun.*, vol. 36, no. 2, pp. 363–375, Feb. 2018.

[4] P. Zhan, K. Yu, and A. L. Swindlehurst, "Wireless relay communications with unmanned aerial vehicles: Performance and optimization," *IEEE Trans. Aerosp. Electron. Syst.*, vol. 47, no. 3, pp. 2068–2085, Jul. 2011.

[5] D. Orfanus, E. P. de Freitas, and F. Eliassen, "Self-organization as a supporting paradigm for military UAV relay networks," *IEEE Commun. Lett.*, vol. 20, no. 4, pp. 804–807, Apr. 2016.

[6] S. Jeong, O. Simeone, and J. Kang, "Mobile edge computing via a UAV-mounted cloudlet: Optimization of bit allocation and path planning," *IEEE Trans. Veh. Technol.*, vol. 67, no. 3, pp. 2049–2063, Mar. 2018.

[7] R. I. Bor-Yaliniz, A. El-Keyi, and H. Yanikomeroglu, "Efficient 3-D placement of an aerial base station in next generation cellular networks," in *Proc. IEEE Int. Conf. Commun.*, Kuala Lumpur, Malaysia, May 2016, pp. 1–5.

[8] J. Lyu, Y. Zeng, R. Zhang, and T. J. Lim, "Placement optimization of UAV-mounted mobile base stations," *IEEE Commun. Lett.*, vol. 21, no. 3, pp. 604–607, Mar. 2017.

[9] M. Mozaffari, W. Saad, M. Bennis, and M. Debbah, "Efficient deployment of multiple unmanned aerial vehicles for optimal wireless coverage," *IEEE Commun. Lett.*, vol. 20, no. 8, pp. 1647–1650, Aug. 2016.

[10] M. Mozaffari, W. Saad, M. Bennis, and M. Debbah, "Unmanned aerial vehicle with underlaid device-to-device communications: Performance and tradeoffs," *IEEE Trans. Wireless Commun.*, vol. 15, no. 6, pp. 3949–3963, Jun. 2016.

[11] M. Chen, M. Mozaffari, W. Saad, C. Yin, M. Debbah, and C. S. Hong, "Caching in the sky: Proactive deployment of cache-enabled unmanned aerial vehicles for optimized quality-of-experience," *IEEE J. Sel. Areas Commun.*, vol. 35, no. 5, pp. 1046–1061, May 2017.

[12] N. Zhao, F. Cheng, F. R. Yu, J. Tang, Y. Chen, G. Gui, and H. Sari, "Caching UAV assisted secure transmission in hyper-dense networks based on interference alignment," *IEEE Trans. Commun.*, vol. 66, no. 5, pp. 2281–2294, May 2018.

[13] D. Yang, Q. Wu, Y. Zeng, and R. Zhang, "Energy trade-off in ground-to-UAV communication via trajectory design," *IEEE Trans. Veh. Technol*, vol. 67, no. 7, pp. 6721–6726, Jul. 2018.

[14] J. Lyu, Y. Zeng, and R. Zhang, "Spectrum sharing and cyclical multiple access in UAV-aided cellular offloading," in *Proc. IEEE GLOBECOM*, Singapore, Dec. 2017, pp. 1–6.

[15] Y. Zeng, R. Zhang, and T. J. Lim, "Throughput maximization for UAV-enabled mobile relaying systems," *IEEE Trans. Commun.*, vol. 64, no. 12, pp. 4983–4996, Dec. 2016.

[16] Y. Zeng and R. Zhang, "Energy-efficient UAV communication with trajectory optimization," *IEEE Trans. Wireless Commun.*, vol. 16, no. 6, pp. 3747–3760, Jun. 2017.

[17] Q. Wu, Y. Zeng, and R. Zhang, "Joint trajectory and communication design for multi-UAV enabled wireless networks," *IEEE Trans. Wireless Commun.*, vol. 17, no. 3, pp. 2109–2121, Mar. 2018.

[18] X. Liu, Z. Li, N. Zhao, W. Meng, G. Gui, Y. Chen, and F. Adachi, "Transceiver design and multihop D2D for UAV IoT coverage in disasters," *IEEE Internet Things J.*, vol. 6, no. 2, pp. 1803–1815, Apr. 2019, doi: 10.1109/JIOT.2018.2877504.

[19] K. Mase and H. Okada, "Message communication system using unmanned aerial vehicles under large-scale disaster environments," in *Proc. IEEE 26th Annu. Int. Symp. Pers., Indoor, Mobile Radio Commun. (PIMRC)*, Hong Kong, Aug./Sep. 2015, pp. 2171–2176.

[20] M. Erdelj and E. Natalizio, "UAV-assisted disaster management: Applications and open issues,"in *Proc. ICNC*, Kauai, HI, USA, Feb. 2016, pp. 1–5.

[21] D. G. Reina, S. L. Toral, and H. Tawfik, "UAVs deployment in disaster scenarios based on global and local search optimization algorithms," in *Proc. 9th Int. Conf. Develop. eSyst. Eng.(DeSE)*, Liverpool, U.K, Aug. 2016, pp. 197–202.

[22] E. Christy, R. P. Astuti, B. Syihabuddin, B. Narottama, O. Rhesa, and F. Rachmawati, "Optimum UAV flying path for device-to-device communications in disaster area," in *Proc. ICSigSys*, Sanur, Indonesia, May 2017, pp. 318–322.

[23] M. Mozaffari, W. Saad, M. Bennis, and M. Debbah, "Mobile unmanned aerial vehicles (UAVs) for energy-efficient Internet of Things communications," *IEEE Trans. Wireless Commun.*, vol. 16, no. 11, pp. 7574–7589, Nov. 2017.

[24] N. H. Motlagh, M. Bagaa, and T. Taleb, "UAV-based IoT platform: A crowd surveillance use case," *IEEE Commun. Mag.*, vol. 55, no. 2, pp. 128–134, Feb. 2017.

[25] H. Wang, J. Wang, G. Ding, L. Wang, T. A. Tsiftsis, and P. K. Sharma, "Resource allocation for energy harvesting-powered D2D communication underlaying UAV-assisted networks," *IEEE Trans. Green Commun. Netw.*, vol. 2, no. 1, pp. 14–24, Mar. 2018.

[26] H. Wang, J. Wang, G. Ding, J. Chen, Y. Li, and Z. Han, "Spectrum sharing planning for full-duplex UAV relaying systems with underlaid D2D communications," *IEEE J. Sel. Areas Commun.*, vol. 36, no. 9, pp. 1986–1999, Sep. 2018.

[27] F. Zhou, Y. Wu, R. Q. Hu, and Y. Qian, "Computation rate maximization in UAV-enabled wireless-powered mobile-edge computing systems," *IEEE J. Sel. Areas Commun.*, vol. 36, no. 9, pp. 1927–1941, Sep. 2018.

[28] A. A. Khuwaja, Y. Chen, N. Zhao, M.-S. Alouini, and P. Dobbins, "A survey of channel modeling for UAV communications," *IEEE Commun. Surveys Tuts.*, vol. 20, no. 4, pp. 2804–2821, 4th Quart., 2018.

[29] Q. Yu, C. Han, L. Bai, J. Choi, and X. Shen, "Low-complexity multi-user detection in millimeter-wave systems based on opportunistic hybrid beamforming," *IEEE Trans. Veh. Technol.*, vol. 67, no. 10, pp. 10129–10133, Aug. 2018.

[30] Z. Xiao, P. Xia, and X.-G. Xia, "Enabling UAV cellular with millimeter-wave communication: Potentials and approaches," *IEEE Commun. Mag.*, vol. 54, no. 5, pp. 66–73, May 2016.

[31] H. Nishiyama, M. Ito, and N. Kato, "Relay-by-smartphone: Realizing multihop device-to-device communications," *IEEE Commun. Mag.*, vol. 52, no. 4, pp. 56–65, Apr. 2014.

[32] M. M. Selim, M. Rihan, Y. Yang, L. Huang, Z. Quan, and J. Ma, "On the outage probability and power control of D2D underlaying noma UAV-assisted networks," *IEEE Access*, vol. 7, pp. 16525–16536, 2019.
[33] D. Feng, L. Lu, Y. Yuan-Wu, G. Y. Li, G. Feng, and S. Li, "Device-to-device communications underlaying cellular networks," *IEEE Trans. Commun.*, vol. 61, no. 8, pp. 3541–3551, Aug. 2013.
[34] X. Lin, J. G. Andrews, and A. Ghosh, "Spectrum sharing for device-to-device communication in cellular networks," *IEEE Trans. Wireless Commun.*, vol. 13, no. 12, pp. 6727–6740, Dec. 2014.
[35] Y. Zhang, Y. Yang, and L. Dai, "Energy efficiency maximization for device-to-device communication underlaying cellular networks on multiple bands," *IEEE Access*, vol. 4, pp. 7682–7691, 2016.
[36] M. Haenggi, *Stochastic Geometry for Wireless Networks*. Cambridge, U.K.: Cambridge Univ. Press, 2012.
[37] M. Haenggi and R. K. Ganti, "Interference in large wireless networks," *Found. Trends Netw.*, vol. 3, no. 2, pp. 127–248, 2009.
[38] A. Al-Hourani, S. Kandeepan, and A. Jamalipour, "Modeling air-to-ground path loss for low altitude platforms in urban environments," in *Proc. IEEE Global Commun. Conf. (GLOBECOM)*, Austin, TX, USA, Dec. 2014, pp. 2898–2904.
[39] E. Bjornson, L. Sanguinetti, J. Hoydis, and M. Debbah, "Optimal design of energy-efficient multi-user MIMO systems: Is massive MIMO the answer?" *IEEE Trans. Wireless Commun.*, vol. 14, no. 6, pp. 3059–3075, Jun. 2015.

MOHAMED RIHAN received the B.Sc. degree (Hons.) in electronics and communication engineering from Menoufia University, Egypt, and the M.Sc. and Ph.D. degrees in electronics and communication engineering from the Egypt-Japan University of Science and Technology, in 2012 and 2015, respectively. From 2014 to 2015, he was a Researcher with the Department of Advanced Information Technology, Graduate School of ISEE, Kyushu University, Japan. From 2016 to 2017, he was an Adjunct Professor with the Center of Photonics and Smart Materials, Zewail City of Science and Technology, Egypt. He was a Postdoctoral Research Fellow with the College of Information Engineering, Shenzhen University, China, from March 2017 to March 2019. He joined the School of Mathematics and Statistics, Shenzhen University, in April 2019. He is also serving as an Assistant Professor with the Faculty of Electronic Engineering, Menoufia University, Egypt. His current research interests include UAV-assisted communications, fog computing access networks, massive MIMO and mmWave communications, interference alignment, resource allocation, cognitive heterogeneous networks, and the applications of signal processing in wireless communications.

MAHMOUD M. SELIM received the B.Sc. degree (Hons.) in electronics and electrical communications engineering from the Faculty of Engineering, Tanta University, Egypt, and the M.Sc. and Ph.D. degrees in electronics and communication engineering from the Egypt-Japan University of Science and Technology (E-JUST), in 2012 and 2015, respectively. From 2014 to 2015, he was a Researcher with the Department of Advanced Information Technology, Graduate School of ISEE, Kyushu University, Japan. Since 2015, he has been an Assistant Professor with the Department of Electronics Engineering and Electrical Communications, Faculty of Engineering, Tanta University, Egypt. He is currently a Postdoctoral Research Fellow with the College of Information Engineering, Shenzhen University, China. His current research interests include radio resource allocation for 5G heterogeneous networks, 5G new multicarrier modulation waveforms, massive MIMO precoding and detection, non-orthogonal multiple access, and the applications of signal processing in wireless communications.

CHEN XU received the B.S. and M.S. degrees from Xidian University, Xi'an, China, in 1986 and 1989, respectively, and the Ph.D. degree from Xi'an Jiaotong University, Xi'an, in 1992.

In 1992, he joined Shenzhen University, Shenzhen, China. From 1999 to 2000, he was a Research Fellow with Kansai University, Suita, Japan. From 2002 to 2003, he was a Research Fellow with the University of Hawaii at Mānoa, Honolulu, HI, USA. He is currently a Professor with Shenzhen University. His current research interests include image processing, intelligent computing, and wavelet analysis.

LEI HUANG (M'07–SM'14) was born in Guangdong, China. He received the B.Sc., M.Sc., and Ph.D. degrees in electronic engineering from Xidian University, Xi'an, China, in 2000, 2003, and 2005, respectively.

From 2005 to 2006, he was a Research Associate with the Department of Electrical and Computer Engineering, Duke University, Durham, NC, USA. From 2009 to 2010, he was a Research Fellow with the Department of Electronic Engineering, City University of Hong Kong, and a Research Associate with the Department of Electronic Engineering, The Chinese University of Hong Kong. From 2011 to 2014, he was a Professor with the Department of Electronic and Information Engineering, Harbin Institute of Technology Shenzhen Graduate School. Since November 2014, he has been with the College of Information Engineering, Shenzhen University, where he is currently a Distinguished Professor and the Director of the Shenzhen Key Laboratory of Advanced Navigation Technology. His current research interests include array signal processing, statistical signal processing, sparse signal processing and their applications in radar, navigation, and wireless communications.

He is an Elected Member of Sensor Array and Multichannel (SAM) Technical Committee (TC) of the IEEE Signal Processing Society, and an IET Fellow, in 2018. He is currently on the Editorial Boards of the IEEE TRANSACTIONS ON SIGNAL PROCESSING, *Digital Signal Processing*, and *IET Signal Processing*.